Talanta 280 (2024) 126598

Contents lists available at ScienceDirect

Talanta

journal homepage: www.elsevier.com/locate/talanta

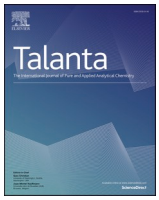

Electrochemical behaviour of poly(amidoamine) dendrimers at micropipette-based liquid/liquid micro-interfaces

Gazi Jahirul Islam [a,b], Damien W.M. Arrigan [a,*]

[a] School of Molecular and Life Sciences, Curtin University, GPO Box U1987, Perth, WA 6845, Australia
[b] Department of Chemistry, University of Barishal, Barishal, 8254, Bangladesh

ARTICLE INFO

Keywords:
Poly(amidoamine) dendrimers
Micropipette
Ion-transfer
Voltammetry
μITIES

ABSTRACT

Dendrimers are macromolecules with well-defined three-dimensional structures, sizes and surface charges. In this work, four generations of poly(amidoamine) (PAMAM) dendrimers were investigated at the micro-interface between two immiscible electrolyte solutions (μITIES) to understand their electrochemical responses as simple models of ionised macromolecules. Cyclic voltammetry (CV) across a range of aqueous phase pH revealed that all four generations (G0-G3) presented diffusion-controlled ion-transfer from aqueous to organic phase, while the reverse transfers from organic to aqueous phase varied with both pH and the dendrimer generation. The larger dendrimers (G2 and G3) show an adsorption behaviour at pH $\leq$ 3.5, but show a diffusional response at pH $\geq$ 6. On the other hand, the smaller dendrimers (G0 and G1) always show a diffusional response and are not impacted by the pH. This indicates that more highly charged dendrimers condense at the interface. The reverse scan of CVs showed that an increased applied potential was required to remove (desorb) these polycations from the interfaces in comparison to smaller, less charged species. Diffusion coefficients (D) were estimated, showing a decrease with increasing generation. Limits of detection for these dendrimers by CV at the μITIES were 0.4, 0.2, 0.7 and 0.5 μM for G0 to G3, respectively, while differential pulse voltammetry lowered the LODs (0.07, 0.05, 0.09 and 0.08 μM, respectively). These study shows that the μITIES provides a simple way to detect and evaluate the electrochemical behaviour of ionised macromolecules, providing a simple illustration of detection mechanism with diffusion or adsorption processes.

1. Introduction

Since the 1990s, dendrimers have become popular macromolecules in scientific research. These types of macromolecules were first reported by Vögtle et al. [1], who synthesized branched tripropylamine macromolecules. Subsequently, branched poly(amidoamine) (PAMAM) dendrimers were synthesized by Tomalia et al. [2]. Dendrimers are unique and non-traditional polymers with well-defined structures, sizes and surface charges. They are three-dimensional macromolecules with highly symmetric, spherical, hyper-branched, and monodisperse characteristics that are different from linear polymers [3–9]. In general, a dendrimer is made up of three parts – a core, a scaffold, and a surface. The core is the centre part of the molecule and possessing a given number of dendrons or branches. Each dendron is composed of a number of branching points or scaffold and surface groups [10–13]. The number and nature of functional groups of the dendrimer, which depends on the generation, determines their physical and chemical properties [14].

Due to their special structure, dendrimers have many specific properties like solubility, viscosity, hydrodynamic character, and versatility [10]. Dendrimers are extensively studied for their distinctive features and used in various applications. Due to the possibility for precise control over their physicochemical properties and their branched polymeric properties, dendrimers have been investigated for a wide range of biomedical applications [15–18], such as drug delivery, as unimolecular micelles and protein mimics [19–23], in gene delivery [24–27], in cell membrane interactions [28], and as nanocarriers for RNAi therapeutic cancer treatment [23,27,29–31]. Dendrimers are also used as catalysts [32,33] and self-assembled monolayers as models for biological systems [34,35]. Electroactive dendrimers are of great importance to understand biological electron-transfer processes [36] and they are also used as electron-transfer mediators for sensors or electro-optical devices [37].

Dendrimers such as PAMAM and poly(propylenimine) [PPI] may have cationic, anionic or neutral moieties at their surfaces which are

* Corresponding author.
E-mail address: d.arrigan@curtin.edu.au (D.W.M. Arrigan).

https://doi.org/10.1016/j.talanta.2024.126598
Received 7 May 2024; Received in revised form 16 July 2024; Accepted 19 July 2024
Available online 20 July 2024

mainly responsible for the high solubility, reactivity and toxicity of these molecules [13,38]. PAMAM dendrimers are widely studied in drug-delivery because of their charged or polar characteristics under biological conditions [39,40].

The electrochemical transfer of electrons or ions across the interface between two immiscible electrolyte solutions (ITIES) is a well-established field in electrochemistry [41–43]. The voltammetric response of macromolecules and bio-macromolecules such as DNA and proteins at the ITIES has become a promising tool for their detection. For example, the electrochemical behaviour of insulin [44], haemoglobin [45], myoglobin [46] and cytochrome *c* [47,48] was investigated at the ITIES and enabled elucidation of their electrochemical properties. The electrochemical and physicochemical properties of some dendrimers have been evaluated from their voltammetric behaviour at the water/1, 2-dichloroethane (DCE) ITIES. Nagatani et al. reported [49] that the voltammetric behaviour of 4th generation (G4) PAMAM at a water/DCE ITIES was dependent on pH and on the concentrations of both the dendrimer and the organic electrolyte. Analysis of the interfacial response mechanism by potential modulated fluorescence (PMF) spectroscopy showed that at pH 7 the dendrimer transferred across the interface and adsorbed at the organic side of the interface. Nagatani et al. also studied dendrigraft poly-l-lysines and their interactions with an anionic fluorescent probe, 8-anilino-1-naphthalenesulfonate. Transfer of the probe from its complex with the dendrigraft to the organic phase was determined, whereas the dendrigraft adsorbed at the interface, as revealed by in situ fluorescence spectroscopy [50]. This group also demonstrated that the anthracycline antibiotics, daunorubicin (DNR) and doxorubicin (DOX), exhibited specific interactions with amphoteric phospholipid layers and carboxylate-terminated PAMAM dendrimers at a water/DCE ITIES [51]. Calderon et al. [52] analysed a series of carbosilane dendrimers with cationic imidazolium surface groups where they proposed an interfacial ion transfer process, depending on the nature of the species. Herzog et al. [53] investigated the electrochemical response, sensitivity and detection limit of four poly-l-lysine dendrigrafts (G2-G5) at the water/DCE ITIES and found that the limit of detection decreased (from 11 to 0.65 μM) and the sensitivity increased (from 1.8 to 25.8 μA μM^{-1}) with increasing generation from G2 to G5. Herzog's group [54] further investigated the effects of silica modified μITIES arrays on the electrochemical behaviour of PAMAM generations G0 and G1. They found that the multi-cationic dendrimers had an electrostatic interaction with the negatively charged silica deposited at the interface. More recently, Shao's group [55] investigated the facilitated ion transfer (FIT) of PAMAM (G0–G2) by dibenzo-18-crown-6 (DB18C6) at a water/DCE μITIES, where they found that the facilitated transfer potential of PAMAM decreased with increasing DB18C6 concentration. They also proposed that the higher generation dendrimers might transfer at the interface through a deprotonation process. Kowalewska et al. studied a series of carbosilane dendrimers that had positively charged imidazolium groups on their surfaces. They found that these ionised macromolecules underwent interfacial transfer accompanied by adsorption/desorption [56]. Previously, Arrigan's group [57] reported on the analysis of different generations of PPI and PAMAM dendrimers at a water/DCE ITIES. They found that the electrochemical behaviour depended on the dendrimer family, the generation number, and the experimental pH. They also observed that the lower generations gave well-defined responses for both dendrimer families, whereas the higher generations showed distorted voltammograms and instability of the interface. That study was undertaken at macro-ITIES, i.e. millimetre-centimetre sized interfaces. The use of a μITIES, such as formed at the mouth of a micropipette, should provide improved voltammograms for higher generation PAMAM and hence better electrochemical analysis.

In this study, the electrochemical behaviour of four generations of PAMAM dendrimers (generations 0–3, G0–G3) at single μITIES formed at the tip of glass pipettes were investigated. Previous studies used large ITIES, so results might be influenced by uncompensated resistance or capacitance effects. A single μITIES minimises these effects [43,58–60] and enables observation of unexpected electrochemical behaviour. Finally, the interest in dendrimers is important because they are ideal macromolecules which can be ionised easily by adjusting the aqueous phase pH. Hence, they serve as model macromolecules that might reveal new information about the electrochemistry of (bio)macromolecules at the μITIES. The PAMAM dendrimers studied here are non-redox-active and their electrochemistry at the ITIES depends on their acid-base behaviour. The pKa of the primary amine groups within PAMAM dendrimers is 9.5 [28] and their tertiary amine groups are fully protonated only at pH 3 [29]. As a result, it is expected that at higher pH, only the primary amines will be protonated, whilst at sufficiently low pH, all tertiary amino groups are protonated. Hence, the PAMAM dendrimers are expected to interact differently with the interface, depending on the pH of the aqueous phase. For this reason, a wide range of aqueous phase pH (1.75–11.0) was examined for all four PAMAM generations to determine the impact of pH on their electrochemical behaviour.

2. Experimental

2.1. Reagents

All the reagents were purchased from Sigma-Aldrich Australia Ltd. and used as received unless otherwise indicated. The organic electrolyte bis(triphenylphosphoranylidene)-ammonium tetrakis(4-chlorophenyl) borate (BTPPATPBCl) was prepared by metathesis of equimolar amounts of bis(triphenylphosphoranylidene)ammonium chloride (BTPPACl) and potassium tetrakis(4-chlorophenyl)borate (KTPBCl) [61]. BTPPATPBCl (0.01 M) solutions were prepared in 1,2-dichloroethane (DCE). Chlorotrimethylsilane was used for silanization of pipettes. Tetraethylammonium (TEA^+) was used as a model ion to characterize the pipettes. All aqueous solutions (e.g. LiCl solution) were prepared in purified water from a USF Purelab plus UV (resistivity: 18.2 MΩ cm). The PAMAM dendrimer kits (generations G0 - G3) were purchased from Sigma-Aldrich Australia Ltd.

2.2. Fabrication of micropipettes

Micropipettes were prepared from borosilicate capillaries (O.D. 1.0 mm; I.D. 0.75 mm) using a P2000 laser pipette puller (Sutter Instruments), as described previously [62]. The five programmable parameters used were: heat (270), filament (3), velocity (20), delay (220), and pull (165). After pulling, the inner surfaces of the pipettes were silanised with chlorotrimethylsilane in a simple vaporization process [62]. Pipette tips were gently abraded on a clean surface, visually inspected using an optical microscope, and characterized by ion-transfer cyclic voltammetry (Fig. S1). Stable voltammograms indicated a pipette suitable for experiments. Pipette radii were calculated from the steady-state current for the transfer of TEA^+ ions from the outer (aqueous) solution to the inner (DCE) solution (Fig. S2) using equation S1.

2.3. Electrochemical cell

Electrochemical measurements were conducted using an Autolab PGSTAT302 N electrochemical analyser (Metrohm Autolab, Utrecht, The Netherlands) with NOVA software. The organic electrolyte phase was introduced into the pipette and the organic reference solution (saturated BTPPACl in 10 mM LiCl) was placed on the top of the organic phase. Then the pipette was immersed into the aqueous phase so that an ITIES formed at the tip of the pipette. A two-electrode cell was employed with one Ag/AgCl electrode in the aqueous solution and another Ag/AgCl electrode in the organic reference solution. All voltammograms are reported as the recorded potentials versus the Ag/AgCl reference electrode. Unless stated otherwise, the cyclic voltammetry (CV) scan rate was 10 mVs^{-1}. For differential pulse voltammetry (DPV), the

conditioning potential, equilibrium time, step potential, modulation amplitude, modulation time and interval time were 0.1 V, 30 s, 0.005 V, 0.05 V, 0.04 s and 0.5 s, respectively. The pH of the aqueous LiCl solution was adjusted by addition of NaOH and HCl solutions and measured using a calibrated pH meter (model CP-511, Ionode, Queensland, Australia). The cell composition is as follows:

3. Results and discussion

3.1. Origin of the CV response

The electrochemical behaviour of PAMAM dendrimers at the μITIES between water and DCE formed at the tip of a glass micropipette were studied by CV. The CVs start from low potential and scan towards more positive potentials. On the forward scan, a sigmoidal voltammetric wave formed (Fig. 1) at higher potential (near to the background electrolyte transfer), corresponding to transfer of the dendrimer G0, and indicates radial diffusion from the outer aqueous phase to the micro-interface. On the other hand, a peak-shaped response was evident on the reverse scan (Fig. 1), indicating linear diffusion of dendrimers within the inner DCE phase to the interface [42]. A similar response was obtained for the model ion TEA^+ (Fig. S1). Background subtraction of the blank voltammogram from the dendrimer voltammogram clearly accentuates the sigmoidal voltammogram on the forward scan (Fig. 1). The shape of the voltammogram illustrates the possible charge transfer mechanism for dendrimer behaviour at the ITIES, i.e. radial diffusion-controlled transfer of the ionised dendrimer from the aqueous phase outside the pipette to the organic phase inside the pipette. All four generations of dendrimers produced similar CV responses (Figure S3-Figure S6) and formed well-defined voltammograms, with the extent of ion transfer current varying consistently with concentration and aqueous phase pH.

It is possible that the transfer process involve cationic dendrimer interacting with organic phase anion at the interface, as reported for protein electrochemistry at the ITIES [45,63]. If the formation of a complex between cation of the dendrimer and anion of the organic electrolyte is limited by arrival of organic anion at the interface, a voltammetric peak on the forward scan would be expected, due to linear diffusion of the organic anion within the inner (DCE) phase. However, steady-state voltammograms were obtained (Fig. 1, Figs. S3–S6), which suggests the controlling mass transport process was in the aqueous phase, and hence supports the conclusion that dendrimer transfer occurred.

Table 1 shows the hydrodynamic diameters and the numbers of primary and secondary amino groups of these dendrimers [64,65]. As the amino groups can be ionised, the molecular charge of the dendrimers depends on the experimental pH of dendrimer solution. The approximate molecular charges (z_i) of these dendrimers based on acid-base titrations [39] are summarised in Table 1. Protonation of PAMAM dendrimers first occurs at the primary amino surface groups at the outer rim of the dendrimers at high pH. Subsequently, the interior tertiary amino groups are protonated at lower pH and the central tertiary amines are protonated at even lower pH [39,57].

3.2. CV of PAMAM dendrimer G0

PAMAM dendrimer G0 has four surface primary amino groups and two interior tertiary amino groups [64]. Fig. 1 shows the typical CVs before and after background subtraction. Fig. 2 shows the background subtracted CVs of G0 in different aqueous phase pH. The shape of the CVs are similar, which indicates that the overall transfer behaviour of G0

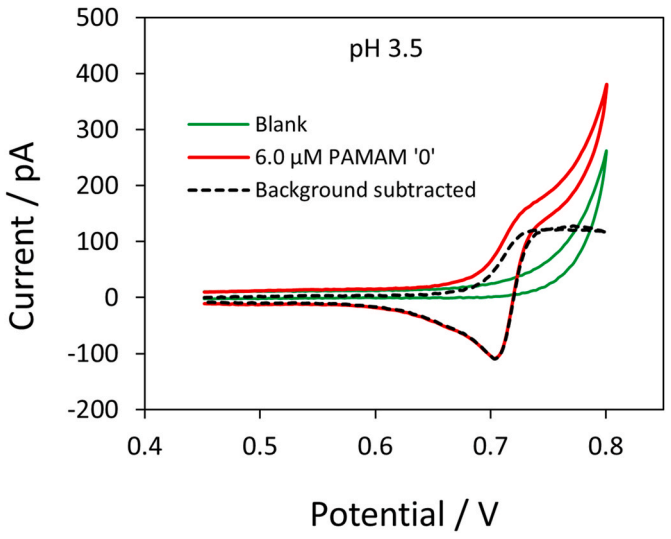

Fig. 1. CVs of 6 μM PAMAM G0 transfer without (red, solid line) and with (black, dashed line) background subtraction at a μITIES formed at a micropipette tip (radius 8.8 μm). CV of blank (green, solid line) is also shown.

at different pH is the same except and only the magnitude of response changes. The change of current with pH is due to the different charges of G0 at different pH. For this case, the best response was at pH 3.5 and the variation in the shape of the CVs may be because of the different shape of the pipettes. The responses in acidic pH aqueous phases are consistent.

Fig. 2g and h shows the current versus concentration plots for both forward and reverse scans at different pH. It shows that if we decrease the pH from the un-adjusted LiCl solution (pH 6.0), then initially the current response increased and gives the highest response at pH 3.5. Then it gradually decreased and no response was seen at very low pH of 1.75 (Fig. 2a). On the other hand, the current response is always low at higher pH than pH 6.0 (Fig. 2e and f). The current response normally depends on the ionised charge of the dendrimers, which varies with pH [39]. With the decrease of pH the charge of the dendrimers increase and with the increase of pH, the charge decreases. This is because the surface and inner amino groups become more protonated at lower pH and vice versa for higher pH (Table 1) [39]. The charges (z_i) of G0 at pH 9, 6, 3.5 and 2.75 are 2, 5, 6 and 6 respectively [39]. Accordingly, it is aligned with the experiment that as pH decreases from 9 to 3.5, the current increased. But for lower the pH, the current decreased further although G0 is fully protonated, which is unexpected. The half-wave potential ($E_{1/2}$) and peak potential (E_p) for the transfer of G0 at the liquid/liquid micro-interface was assessed at different pH. The $E_{1/2}$ based on the forward scan are 0.71, 0.71, 0.7 and 0.69 V and E_p for the reverse scan are 0.71, 0.71, 0.7 and 0.69 V for pH 2.75, 3.5, 6.0 and 9.0, respectively (Table 2). Interestingly, no difference between $E_{1/2}$ and E_p has been seen and both potentials essentially remain the same with the increase of concentrations within each pH (Fig. S3).

3.3. CV of PAMAM dendrimer G1

PAMAM dendrimer G1 has eight surface primary amino groups and six interior tertiary amine groups (Table 1) [64]. Fig. 3 shows the background subtracted CVs of G1 at different aqueous phase pH. Between pH 1.75 and 6.0, the charge of G1 is 14 and then the charge decreases with increasing pH (Table 1) [39].

Fig. 3i and j shows the current verses concentration plots for forward

$$\mathrm{Ag}\,|\,\mathrm{AgCl}\,|\,\begin{matrix}\text{Sat'd BTPPACl}\\ \text{in 10 mM LiCl}\end{matrix}\,|\,\begin{matrix}\text{10 mM BTPPATPBCl}\\ \text{in DCE}\end{matrix}\,||\,\begin{matrix}\text{x μM PAMAM in 10 mM}\\ \text{LiCl of adjusted pH}\end{matrix}\,|\,\mathrm{AgCl}\,|\,\mathrm{Ag}$$

Table 1
Structural characteristics of different generations of PAMAM dendrimers and their charges at different pH [39,64,65].

Dendrimer Generations	Hydro- dynamic diameter (nm)	Number of amino groups		Charge (z_i) of the ionised macromolecule at different pH							
		Primary	Secondary	pH 1.75	pH 2.25	pH 2.75	pH 3.5	pH 6.0	pH 9.0	pH 10.0	pH 11.0
G0	1.5	4	2			6	6	5	2		
G1	2.2	8	6	14	14	14	14	9	4	1	
G2	2.9	16	14	30	30	30	20	15	9	3	1
G3	3.6	32	30	62	62	62	60	37	20	4	2

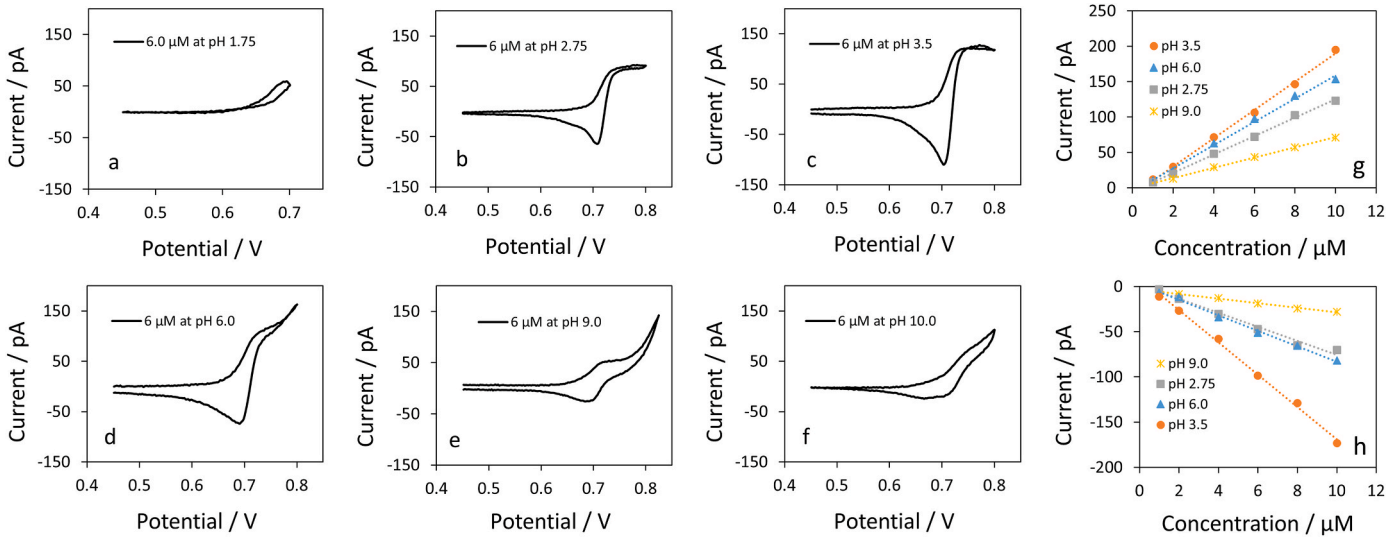

Fig. 2. Background subtracted CVs of PAMAM dendrimer G0 at **(a)** pH 1.75 **(b)** pH 2.75 **(c)** pH 3.5 **(d)** pH 6.0 **(e)** pH 9.0 and **(f)** pH 10.0 with 8.8 µm pipette radius. Figure also shows current vs concentration at pH 2.75, 3.5, 6.0 and 9.0 for **(g)** forward scan and **(h)** reverse scan.

Table 2
Values of the slope of the current vs concentration calibration curve and of ion-transfer potentials of PAMAM dendrimer generations G0 to G3 at different pH.

	Dendrimer generations		pH **1.75**	pH **2.25**	pH **2.75**	pH **3.5**	pH **6.0**	pH **9.0**	pH **10.0**	pH **11.0**
Slope pA/µM	G0	forward			13.1	20	16.4	7.2		
		reverse			−7.8	−17.9	−8.6	−2.6		
	G1	forward	17.2	17.7	20.1	25.8	20.1	10.9		
		reverse	−12.1	−12.3	−18.3	−29.3	−22.7	−8.73		
	G2	forward	41.3	38.2	30.4	14.8	22.2	25.3	28.6	33.6
		reverse	−124	−121	−33.2	−22.1	−29.9	−38.4	−41.7	−37.7
	G3	forward	48.9	33.9	75.8	62.6	44.2	50.6	39.7	35.7
		reverse	−214	−173	−339	−230	−148	−200	−170	−70.0
Ion-transfer Potential (V) vs. Ag/AgCl	G0	$E_{1/2}$			0.71	0.71	0.70	0.69		
		E_p			0.71	0.71	0.70	0.69		
	G1	$E_{1/2}$	0.67	0.67	0.67	0.67	0.67	0.67		
		E_p	0.67	0.67	0.67	0.67	0.67	0.67		
	G2	$E_{1/2}$	0.65	0.66	0.69	0.69	0.66	0.67	0.67	0.74
		E_p	0.63	0.63	0.63	0.63	0.65	0.65	0.67	0.71
	G3	$E_{1/2}$	0.66	0.65	0.70	0.70	0.68	0.66	0.69	0.74
		E_p	0.61	0.60	0.60	0.61	0.61	0.62	0.64	0.72

and reverse scans respectively, at the various pH studied. Similar responses for PAMAM G0 were observed, as the protonation of amino groups in G1 follows the same pattern. Table 1 shows that there is no charge at pH 11.0, consistent with the CV response (Fig. 3h). As the pH decreased, the charges increased and G1 became fully protonated at pH 3.5 and lower [39]. The CVs also follow this pattern, with the highest current response at pH 3.5. However, below pH 3.5, the current response gradually decreased, similar to G0, although they are fully charged. The half-wave potential ($E_{1/2}$) and peak potential (E_p) for the transfer of G1 at the liquid/liquid micro-interface did not change with pH. The measured $E_{1/2}$ based on the forward scan is 0.67 V and E_p for the reverse scan is also 0.67 V for all pH (Table 2). Similar to G0, there is no difference between the $E_{1/2}$ and E_p values and these remain constant with increasing concentration (Fig. S4). It is noticeable that in the reverse CV scan there is a second peak at lower pH 1.75 and 2.25 (Fig. S4), which may indicate a process such as adsorption/desorption in addition to the diffusion-controlled ion-transfer.

3.4. CV of PAMAM dendrimer G2

PAMAM dendrimer G2 has 16 surface primary amino groups and 14 interior tertiary amino groups [64]. Fig. 4a-h shows the background subtracted CVs of G2 across a range of aqueous phase pH values. The shapes of the CV forward scans are similar but the reverse scans here

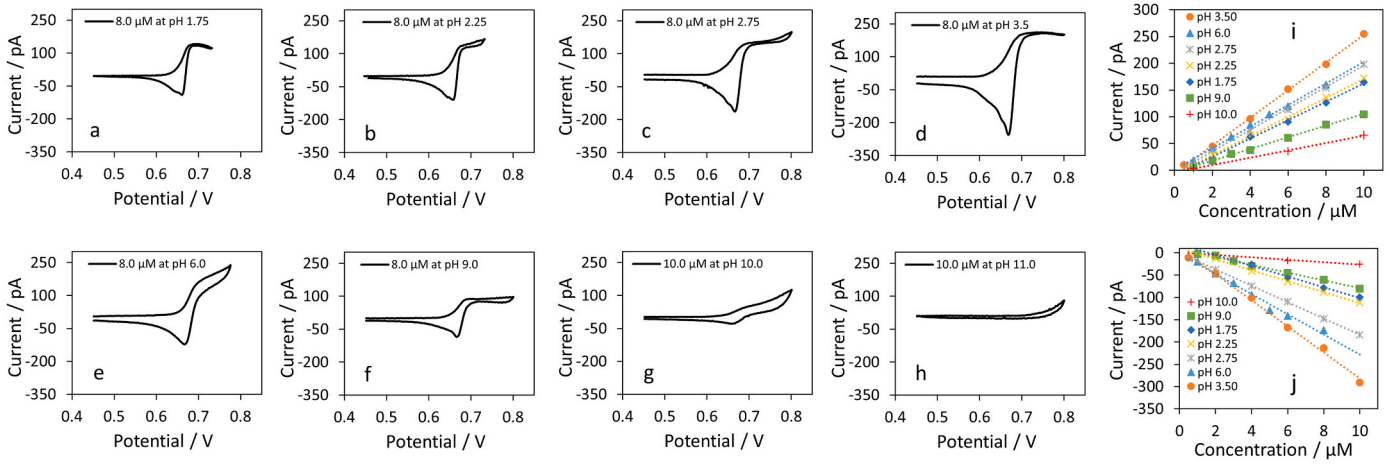

Fig. 3. Background subtracted CVs of 8.0 μM PAMAM dendrimer G1 at **(a)** pH 1.75 **(b)** pH 2.25 **(c)** pH 2.75 **(d)** pH 3.5 **(e)** pH 6.0 **(f)** pH 9.0 and 10 μM G1 at **(g)** pH 10.0 and **(h)** pH 11.0. Pipette radius for (a) to (e) was 9.2 μm and for (f) to (h) was 8.4 μm. Also shown are current vs. concentration plots for G1 at pH 1.75, 2.25, 2.75, 3.5, 6.0, 9.0 and 10.0 for **(i)** forward scan and **(j)** reverse scan.

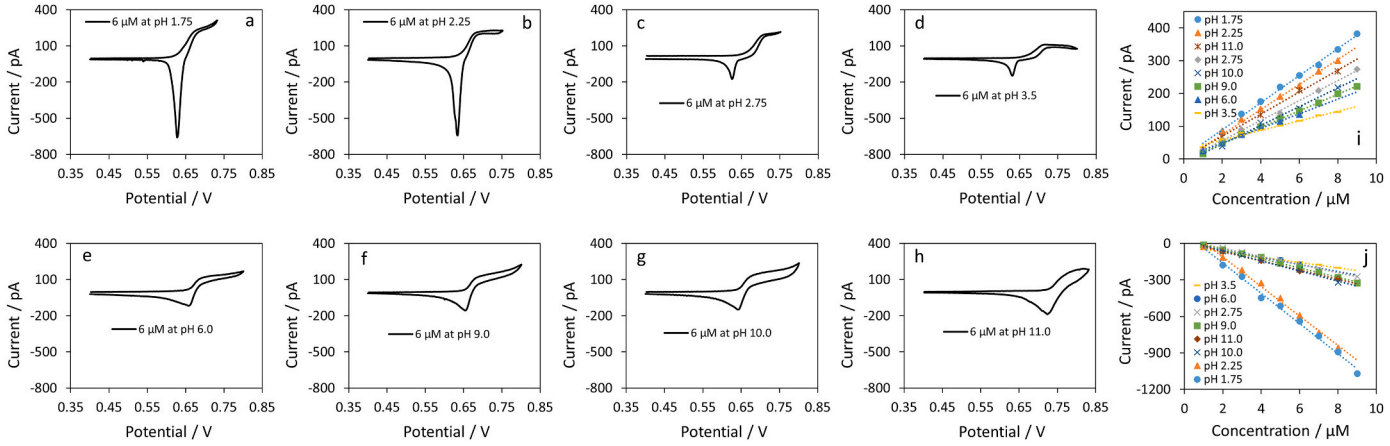

Fig. 4. Background subtracted CVs of 6 μM PAMAM dendrimer G2 at **(a)** pH 1.75 **(b)** pH 2.25 **(c)** pH 2.75 **(d)** pH 3.5 **(e)** pH 6.0 **(f)** pH 9.0, **(g)** pH 10.0 and **(h)** pH 11.0. The pipette radius was 9.5, 8.4, 8.4, 8.4, 8.0, 9.5, 9.5 and 10.3 μm, respectively. Also shown is current vs concentration plots for PAMAM G2 at pH 1.75, 2.25, 2.75, 3.5, 6.0, 9.0, 10.0 and 11.0 for **(i)** forward scan and **(j)** reverse scan.

show a range of behaviours. The charge of ionised G2 at pH 11.0 is 1 [39] and the charge gradually increases with decreasing pH, becoming fully protonated at pH 2.75 and lower, where the charge is 30 [39]. Interestingly, in this case, the current response did not show any particular trend with the ionised molecular charge at and above pH 3.5. Fig. 4i and j shows the current versus concentration plots for both forward and reverse CV scans at different pH. It shows that in both cases of high pH and low pH, G2 gave higher electrochemical responses. The highest response for both forward and reverse scans were at pH 1.75 and pH 2.25. But the reverse peak gave exceptionally high currents for both these pH. However, for G0 at pH 1.75, there was no response and G1 gave little response. The highest response was at pH 3.5 for both G0 and G1. The response for G2 increased with pH up to 11.0 although the ionised charges decreased. On the other hand, G1 yielded a low response at pH 10.0 and no response at pH 11.0, as expected, based on the ionised charges.

From Fig. 4, it is clear that the shape of the reverse peak became sharper pH 3.5 and lower. Based on this voltammetric peak shape, we suggest that G2 undergoes an adsorption process at lower pH. The current also increased within the range pH 6.0 to 11.0, which might be due to adsorption although the ionised charge decreased. On the other hand, Table 2 shows the ion-transfer potential varied with pH in contrast to the behaviour of G0 and G1 (Fig. S5). As the pH increased (1.75–10.0), the ion-transfer potential shifted to higher values. Furthermore, the difference between $E_{1/2}$ and E_p decreased with increasing pH. These variations were insignificant for G0 and G1. This may be because the lower generation dendrimers G0 and G1 show the simplest electrochemistry whereas G2 and higher generations show more complex behaviour due to their molecular sizes and charges.

3.5. CV of PAMAM dendrimer G3

PAMAM dendrimer G3 is a giant molecule with 32 surface primary amino groups and 30 interior tertiary amino groups (Table 1) [64]. CV of G3 showed noticeable differences in behaviour compared to the lower generations. Generally, the reverse scan current responses for G3 were 2–3 times greater than the current on the forward scan. Only at pH 11.0 the reverse peak current is small, but still larger than obtained for the other generations although the ionised molecular charge is only 2 at this pH. The high reverse scan current is attributed to adsorption of ionised macromolecules at the interface. The narrow and enhanced peak shape (Fig. 5) also indicates the role of an adsorption/desorption process, unlike the broad diffusion-controlled processes for TEA^+ ion transfer (Fig. S1), for example. Another important noticeable difference for G3 from the other generations was the difference between forward half-wave potential and reverse peak potential ($E_{1/2}$ - E_p). The reverse

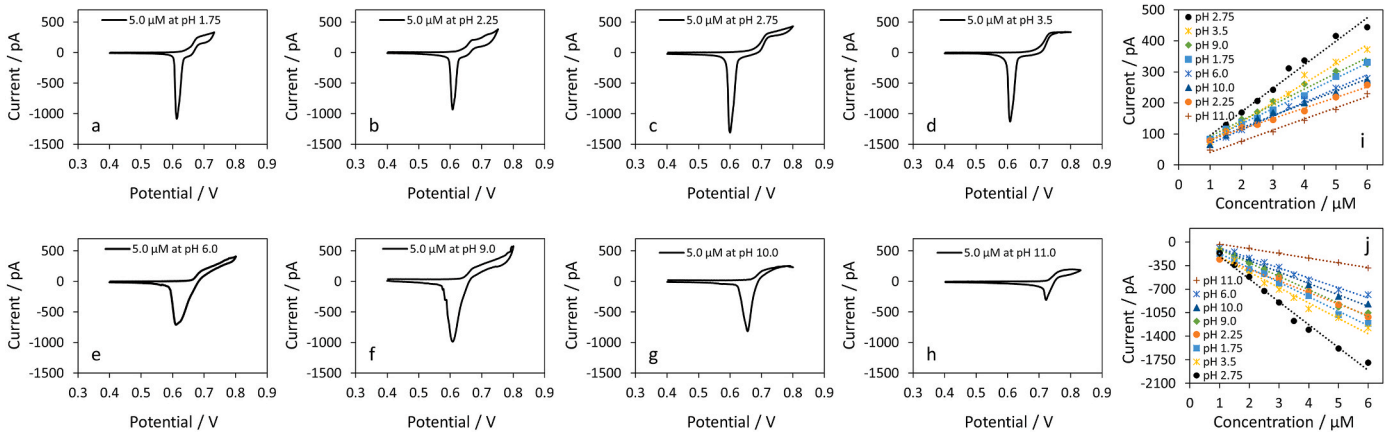

Fig. 5. Background subtracted CVs of 5 μM PAMAM dendrimer G3 at **(a)** pH 1.75 **(b)** pH 2.25 **(c)** pH 2.75 **(d)** pH 3.5 **(e)** pH 6.0 **(f)** pH 9.0, **(g)** pH 10.0 and **(h)** pH 11.0. The pipette radius was 9.5 μm for (a) to (e) and 10.3 μm for (f) to (h). Also shown is current vs. concentration plot for PAMAM G3 at pH 1.75, 2.25, 2.75, 3.5, 6.0, 9.0, 10.0 and 11.0 for **(i)** forward scan and **(j)** reverse scan.

peak is shifted to lower potentials relative to the forward wave, in contrast to G0 and G1. This may be because the ionised macromolecules are attached (adsorbed) more strongly to the interface and thus require additional energy (applied potential) to desorb them from the interface. This distinct behaviour of G3 illustrates the advantages of using a micro-ITIES rather than a macro-interface. Previous studies of PAMAM dendrimers on macro-interfaces did not show the distinctive reverse peak behaviour for higher generations [57]. This interesting behaviour is clearly dependent on PAMAM generation and this may be because as the generation number increased so does the number of ionisable surface and internal functional groups, so that the high positive ionised macromolecular charge increases. At the interface, these highly ionised macromolecule undergo a condensation with charge compensated by electrostatic binding with the anions of the organic phase electrolyte solution. As a result, more highly charged generations have more scope for electrostatic interactions with compensating anions of the organic phase, and stronger complexes are formed as a result. These complexes are neutral (all charges are compensated) and hence adsorption at the interface can occur. Accordingly, these ion-pair complexes require additional energy to remove (desorb) them from the interface [66] and disrupt the complexation. The shift of reverse peak potential is also pH dependent as the shift seems larger at intermediate pH 2.75 to 6.0 and is decreased at lower and higher pH values (Table 2). Fig. 5 shows the overall ion transfer shifts to higher potentials at pH 10 and 11, whereas for other pH values the ion transfers occur at similar potentials. Some of these potential shifts might be due to changes in the aqueous phase reference electrode potential with pH, although this does not impact on the differences in forward and reverse potentials already discussed, i.e. $E_{1/2}$ - E_p. For most cases, the peak potential shifts with the increase of concentration within the same pH (Fig. S6), which also indicates adsorption.

Fig. 5i and j shows the current versus concentration plots for both forward and reverse directions at different pH. It shows that PAMAM generation G3 gives very high electrochemical response at lower pH. The highest response for both forward and reverse directions are obtained at pH 2.75 and pH 3.5. Despite the indication of adsorption, no saturation of the current vs. concentration plot was seen in the range studied here. The electrochemical response at pH 9.0 is also higher than the unadjusted lithium chloride solution (pH 6.0). At higher pH, the response decreased and gave the lowest response at pH 11.0.

3.6. Diffusion coefficients

The diffusion coefficient (D) is an important parameter for electroanalytical investigations as it allows comparison of results to literature values. In this work, the diffusion coefficient was calculated from the steady-state forward current of CVs using the modified Saito equation $I_{ss} = 3.35\pi|z_i|FDCr$ [67]. In this equation, I_{ss} is the steady state current, z_i, *F, D, C* and *r* are the molecular charge, Faraday constant, diffusion coefficient, concentration of species and radius of the interface, respectively. The calculated D values for G0 at pH 2.75, 3.5, 6.0 and 9.0 are 2.5 × 10^{-6}, 3.3 × 10^{-6}, 3.7 × 10^{-6} and 4.1 × 10^{-6} cm^2s^{-1} respectively. D values for G1 are 1.6 × 10^{-6}, 2.0 × 10^{-6}, 2.4 × 10^{-6} and 3.2 × 10^{-6} cm^2s^{-1}; for G2 are 1.2 × 10^{-6}, 0.9 × 10^{-6}, 1.8 × 10^{-6} and 2.9 × 10^{-6} cm^2s^{-1}; and for G3 are 1.3 × 10^{-6}, 1.2 × 10^{-6}, 1.3 × 10^{-6} and 2.5 × 10^{-6} cm^2s^{-1} at pH 2.75, 3.5, 6.0 and 9.0 respectively. These values are consistent with published data. Jiminez et al. determined diffusion coefficients for G0 - G3 by DOSY-NMR spectroscopy in infinite dilution aqueous solution at high and neutral pH. They reported diffusion coefficients of 3.13 × 10^{-6}, 2.14 × 10^{-6}, 1.32 × 10^{-6} and 0.82 × 10^{-6} cm^2s^{-1} for G0-G3, respectively, at pH 7 [68]. Our electrochemically-determined diffusion coefficients at pH 6 are in good agreement with these values. Our electrochemical results also show good agreement with the theoretical estimates made from molecular dynamics simulations, which ranged from 1.2 × 10^{-6} to 3.2 × 10^{-6} cm^2s^{-1} for G1-G3 PAMAM dendrimers [69]. From all of these data, we can see that the diffusion coefficients decrease with increasing generation number, as expected because the diffusion coefficient will decrease with increasing molecular size [68,70]. We found that diffusion coefficient increased with increasing pH, which is also supported by the literature [68].

3.7. Detection limits and sensitivity

The above results show that CV at a micro-ITIES is a useful method to characterize dendrimers of different generations. CV reveals the response mechanism such as diffusion-controlled ion-transfer or adsorption as well as dendrimers' diffusion coefficients (if the response is diffusion-controlled). From a detection or electroanalysis perspective, the limit of detection (LOD) can be estimated from CV. The LODs for G0, G1, G2 and G3 were calculated as 0.4 μM, 0.2 μM, 0.7 μM and 0.5 μM, respectively, at pH 3.5. This pH was chosen because G0 and G1 gave the best responses at this pH. The LOD calculation was based on (3.σ)/S formula [71,72], where S is the slope of the calibration curve and σ is the standard deviation of the y-intercept of the regression line. The sensitivity (slopes) of the CVs for forward and reverse responses are summarised in Table 2. It is interesting to note that for the lower generations (G0 and G1), the ratio of reverse to forward sensitivities are less than 1, indicating that the forward scans are more sensitive to dendrimer concentration. However, for the higher generations, G2 and G3, this ratio

(reverse slope/forward slope) is greater than 1, showing that the reverse peak current is more sensitive to the dendrimer concentration. In fact for generation G2, the ratio is ca. 2 across all the pH studied, while for generation G3, the ratio is ca. 4 across all the pH studied. These results indicate that electrochemical analysis of higher generations of PAMAM dendrimers is best done in acidic conditions and use of a voltammetric scan in which the dendrimer is desorbed from the interface. Finally, to improve the LOD, differential pulse voltammetry (DPV) was investigated, as it is a more sensitive technique. DPV gives sharper and better-defined peaks at a lower concentrations than CV, minimises the influence of the charging current, and gives improved resolution.

DPV was carried out in the forward scan direction because it gave a better response than the reverse direction (Fig. S7). The solution pH for DPV experiments for all PAMAM dendrimers was 3.5. For these experiments, a blank experiment (without analyte) was recorded and then analyte was spiked into the cell from a stock solution. Then, background subtraction was applied. The resulting DPVs are shown in Fig. 6. The LODs calculated from the DPV experiments for G0 to G3 were 0.07 μM, 0.05 μM, 0.09 μM and 0.08 μM, respectively. Therefore, DPV gives nearly 6-times lower LOD compared to CV for G0 detection and 5, 8, and 6 times lower for G1, G2 and G3, respectively. Fig. 6c and d shows that the DPV of G2 and G3 gave a broader peak and develops another small peak, which may be indicative of the adsorption/desorption response seen in CV experiments for the higher generation dendrimers.

4. Conclusions

Electrochemical investigation of four generations of PAMAM dendrimers at the ITIES formed at micropipettes over a wide range of pH was undertaken. In this analysis we focused on how different generations of dendrimers changed their electrochemical properties with pH. Because each dendrimer has amine groups which are protonated at different pH, they are ionised and can be detected by their transfer across the interface. CV of the PAMAM dendrimers provided important information about the transfer response (diffusion-control, adsorption) as well as parameters like diffusion coefficients. CV analysis showed that the transfer from aqueous phase to organic phase was diffusion-controlled for all generations. In contrast, the reverse transfers, from organic to aqueous phase, for G2 and G3 at pH 3.5 or lower followed an adsorption/desorption process and showed diffusion-controlled transfer for pH 6.0 or higher. However, G0 and G1 followed diffusional control for reverse transfers at all pH. Electrochemical responses for G0 and G1 were best at pH 3.5. On the other hand, G2 and G3 show better response at pH 1.75 and 2.75, respectively. Sometimes higher generation dendrimers did not follow a general trend, which may be because their larger sizes and charges makes the response more complex than lower generations. Previous studies also found that sometimes the charges of the higher generation dendrimers were neutralized by electrolyte anions from the aqueous phase which could explain the variation from a general trend [57]. CV analysis provided LODs in the range 0.2–0.7 μM for G0 to G3, whereas DPV enabled improvement of LOD by an order of magnitude, (0.05–0.09 μM) being an improvement on previously published data [57]. The adsorption and desorption of higher generation dendrimers at lower pH may be a result of electrostatic complexation close to the interface; this adsorption/desorption could likewise be used to further improve LODs for dendrimer detection. These results highlight the intriguing opportunities for study of the electrochemical behaviour of ionised dendrimers and other macromolecules at liquid/liquid micro-interfaces.

CRediT authorship contribution statement

Gazi Jahirul Islam: Writing – original draft, Methodology, Investigation, Formal analysis, Conceptualization. **Damien W.M. Arrigan:** Writing – review & editing, Supervision, Resources, Investigation, Conceptualization.

Declaration of competing interest

The authors declare that they have no known competing financial interests or personal relationships that could have appeared to influence the work reported in this paper.

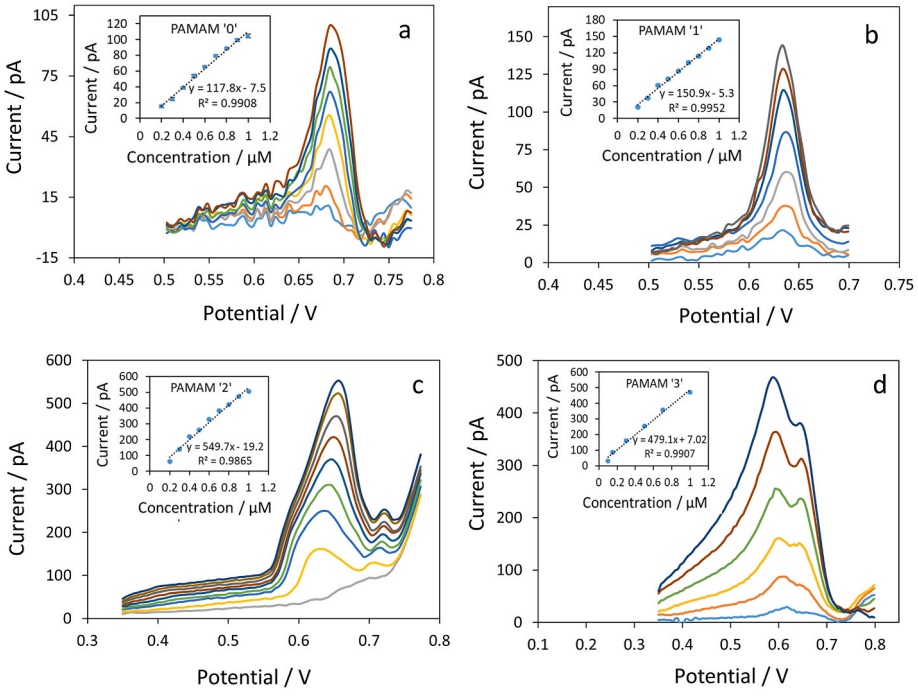

Fig. 6. Background subtracted DPV of **(a)** 0.2, 0.3, 0.4, 0.5, 0.6, 0.7, 0.8 and 0.9 μM PAMAM G0, **(b)** 0.2, 0.3, 0.4, 0.6, 0.8, 0.9 and 1.0 μM PAMAM G1, **(c)** 0.2, 0.3, 0.4, 05, 0.6, 0.7, 0.8, 0.9 and 1.0 μM PAMAM G2, and **(d)** 0.1, 0.15, 03, 0.5, 0.7, and 1.0 μM PAMAM G3, at 9.5 μm, 9.5 μm, 8.4 μm and 8.4 μm radius ITIES, respectively. Insets show current vs concentration plots.

Data availability

Data will be made available on request.

Acknowledgments

GJI gratefully acknowledges the award of a Research Training Programme Scholarship by the Australian Federal Government.

Appendix A. Supplementary data

Supplementary data to this article can be found online at https://doi.org/10.1016/j.talanta.2024.126598.

References

[1] E. Buhleier, W. Wehner, F. Vögtle, Cascade"-and" nonskid-chain-like" syntheses of molecular cavity topologies, Synthesis 1978 (2) (1978) 155–158.
[2] D.A. Tomalia, H. Baker, J. Dewald, M. Hall, G. Kallos, S. Martin, J. Roeck, J. Ryder, P. Smith, A new class of polymers: starburst-dendritic macromolecules, Polym. J. 17 (1) (1985) 117–132.
[3] D.A. Tomalia, J.M. Fréchet, Introduction to “dendrimers and dendritic polymers”, Prog. Polym. Sci. 3 (30) (2005) 217–219.
[4] S. Thakur, P. Kesharwani, R.K. Tekade, N.K. Jain, Impact of pegylation on biopharmaceutical properties of dendrimers, Polymer 59 (2015) 67–92.
[5] P. Kesharwani, R.K. Tekade, N.K. Jain, Generation dependent cancer targeting potential of poly (propyleneimine) dendrimer, Biomaterials 35 (21) (2014) 5539–5548.
[6] B. Birdhariya, P. Kesharwani, N.K. Jain, Effect of surface capping on targeting potential of folate decorated poly (propylene imine) dendrimers, Drug Dev. Ind. Pharm. 41 (8) (2015) 1393–1399.
[7] P. Kesharwani, A.K. Iyer, Recent advances in dendrimer-based nanovectors for tumor-targeted drug and gene delivery, Drug Discov. Today 20 (5) (2015) 536–547.
[8] d.A. Bosman, H. Janssen, E. Meijer, About dendrimers: structure, physical properties, and applications, Chem. Rev. 99 (7) (1999) 1665–1688.
[9] B. Klajnert, M. Bryszewska, Dendrimers: properties and applications, Acta Biochim. Pol. 48 (1) (2001) 199–208.
[10] S.M. Fatemi, S.J. Fatemi, Z. Abbasi, PAMAM dendrimer-based macromolecules and their potential applications: recent advances in theoretical studies, Polym. Bull. (2020) 1–21.
[11] E. Abbasi, S.F. Aval, A. Akbarzadeh, M. Milani, H.T. Nasrabadi, S.W. Joo, Y. Hanifehpour, K. Nejati-Koshki, R. Pashaei-Asl, Dendrimers: synthesis, applications, and properties, Nanoscale Res. Lett. 9 (1) (2014) 1–10.
[12] B. Klajnert, L. Stanisławska, M. Bryszewska, B. Pałecz, Interactions between PAMAM dendrimers and bovine serum albumin, Biochim. Biophys. Acta Protein Proteonomics 1648 (1–2) (2003) 115–126.
[13] P.K. Maiti, T. Çağın, G. Wang, W.A. Goddard, Structure of PAMAM dendrimers: generations 1 through 11, Macromolecules 37 (16) (2004) 6236–6254.
[14] F. Vögtle, G. Richardt, N. Werner, Dendrimer Chemistry: Concepts, Syntheses, Properties, Applications, John Wiley & Sons, 2009.
[15] N.T. Pourianazar, P. Mutlu, U. Gunduz, Bioapplications of poly (amidoamine) (PAMAM) dendrimers in nanomedicine, J. Nanoparticle Res. 16 (4) (2014) 2342.
[16] K. Gardikis, M. Micha-Screttas, C. Demetzos, B. R Steele, Dendrimers and the development of new complex nanomaterials for biomedical applications, Curr. Med. Chem. 19 (29) (2012) 4913–4928.
[17] K. Bezouška, Design, functional evaluation and biomedical applications of carbohydrate dendrimers (glycodendrimers), Rev. Mol. Biotechnol. 90 (3–4) (2002) 269–290.
[18] S.D. Konda, M. Aref, S. Wang, M. Brechbiel, E.C. Wiener, Specific targeting of folate–dendrimer MRI contrast agents to the high affinity folate receptor expressed in ovarian tumor xenografts, Magn. Reson. Mater. Phys. Biol. Med. 12 (2–3) (2001) 104–113.
[19] E. Markatou, V. Gionis, G.D. Chryssikos, S. Hatziantoniou, A. Georgopoulos, C. Demetzos, Molecular interactions between dimethoxycurcumin and Pamam dendrimer carriers, Int. J. Pharm. 339 (1–2) (2007) 231–236.
[20] S. Choudhary, L. Gupta, S. Rani, K. Dave, U. Gupta, Impact of dendrimers on solubility of hydrophobic drug molecules, Front. Pharmacol. 8 (2017) 261.
[21] G.A. Pilkington, J.S. Pedersen, W.H. Briscoe, Dendrimer nanofluids in the concentrated regime: from polymer melts to soft spheres, Langmuir 31 (11) (2015) 3333–3342.
[22] L.J. Twyman, A.E. Beezer, R. Esfand, M.J. Hardy, J.C. Mitchell, The synthesis of water soluble dendrimers, and their application as possible drug delivery systems, Tetrahedron Lett. 40 (9) (1999) 1743–1746.
[23] D. Shcharbin, M. Bryszewska, S. Mignani, X. Shi, J.-P. Majoral, Phosphorus dendrimers as powerful nanoplatforms for drug delivery, as fluorescent probes and for liposome interaction studies: a concise overview, Eur. J. Med. Chem. (2020) 112788.
[24] G.S. Yu, Y.M. Bae, H. Choi, B. Kong, I.S. Choi, J.S. Choi, Synthesis of PAMAM dendrimer derivatives with enhanced buffering capacity and remarkable gene transfection efficiency, Bioconjugate Chem. 22 (6) (2011) 1046–1055.
[25] D. Luong, P. Kesharwani, R. Deshmukh, M.C.I.M. Amin, U. Gupta, K. Greish, A. K. Iyer, PEGylated PAMAM dendrimers: enhancing efficacy and mitigating toxicity for effective anticancer drug and gene delivery, Acta Biomater. 43 (2016) 14–29.
[26] J.D. Eichman, A.U. Bielinska, J.F. Kukowska-Latallo, J.R. Baker Jr., The use of PAMAM dendrimers in the efficient transfer of genetic material into cells, Pharmaceut. Sci. Technol. Today 3 (7) (2000) 232–245.
[27] J. van Haasteren, S.C. Hyde, D.R. Gill, Lessons learned from lung and liver in-vivo gene therapy: implications for the future, Expet Opin. Biol. Ther. 18 (9) (2018) 959–972.
[28] L.J. Fox, R.M. Richardson, W.H. Briscoe, PAMAM dendrimer-cell membrane interactions, Adv. Colloid Interface Sci. 257 (2018) 1–18.
[29] P. Kesharwani, S. Banerjee, U. Gupta, M.C.I.M. Amin, S. Padhye, F.H. Sarkar, A. K. Iyer, PAMAM dendrimers as promising nanocarriers for RNAi therapeutics, Mater. Today 18 (10) (2015) 565–572.
[30] G.M. Pavan, P. Posocco, A. Tagliabue, M. Maly, A. Malek, A. Danani, E. Ragg, C. V. Catapano, S. Pricl, PAMAM dendrimers for siRNA delivery: computational and experimental insights, Chem.–Eur. J. 16 (26) (2010) 7781–7795.
[31] J. Li, S. Xue, Z.-W. Mao, Nanoparticle delivery systems for siRNA-based therapeutics, J. Mater. Chem. B 4 (41) (2016) 6620–6639.
[32] S. Sheikh, M.A. Nasseri, M. Chahkandi, A. Allahresani, O. Reiser, Functionalized magnetic PAMAM dendrimer as an efficient nanocatalyst for new synthesis strategy of xanthene pigments, J. Hazard Mater. (2020) 122985.
[33] Y. Liao, J. Gao, Y. Zhang, Y. Zhou, R. Yuan, W. Xu, Proximity ligation-responsive catalytic hairpin assembly-guided DNA dendrimers for synergistically amplified electrochemical biosensing, Sensor. Actuator. B Chem. 322 (2020) 128566.
[34] M. Zhang, H. Yang, S. Wang, W. Zhang, Q. Hou, D. Guo, F. Liu, T. Chen, X. Wu, J. Wang, PAMAM-based dendrimers with different alkyl chains self-assemble on silica surfaces: controllable layer structure and molecular aggregation, J. Phys. Chem. B 122 (25) (2018) 6648–6655.
[35] K.R. Raghupathi, J. Guo, O. Munkhbat, P. Rangadurai, S. Thayumanavan, Supramolecular disassembly of facially amphiphilic dendrimer assemblies in response to physical, chemical, and biological stimuli, Acc. Chem. Res. 47 (7) (2014) 2200–2211.
[36] K. Inoue, Functional dendrimers, hyperbranched and star polymers, Prog. Polym. Sci. 25 (4) (2000/05/01/, 2000) 453–571.
[37] M.P.G. Armada, J. Losada, M. Zamora, B. Alonso, I. Cuadrado, C.M. Casado, Electrocatalytical properties of polymethylferrocenyl dendrimers and their applications in biosensing, Bioelectrochemistry 69 (1) (2006) 65–73.
[38] J.M. Frechet, D.A. Tomalia, Dendrimers and Other Dendritic Polymers, Wiley, 2001.
[39] D. Cakara, J. Kleimann, M. Borkovec, Microscopic protonation equilibria of poly (amidoamine) dendrimers from macroscopic titrations, Macromolecules 36 (11) (2003) 4201–4207.
[40] Y. Niu, L. Sun, R.M. Crooks, Determination of the intrinsic proton binding constants for poly(amidoamine) dendrimers via potentiometric pH titration, Macromolecules 36 (15) (2003) 5725–5731.
[41] Z. Samec, V. Mareček, J. Koryta, M. Khalil, Investigation of ion transfer across the interface between two immiscible electrolyte solutions by cyclic voltammetry, J. Electroanal. Chem. Interfacial Electrochem. 83 (2) (1977) 393–397.
[42] H. Girault, Charge transfer across liquid—liquid interfaces, Mod. Aspect. Electrochem. 25 (1993) 1–62.
[43] H.D. Jetmore, E.S. Anupriya, T.J. Cress, M. Shen, Interface between Two Immiscible Electrolyte Solutions Electrodes for Chemical Analysis, ACS Publications, 2022.
[44] S. O'Sullivan, E. Alvarez de Eulate, Y.H. Yuen, E. Helmerhorst, D.W.M. Arrigan, Stripping voltammetric detection of insulin at liquid–liquid microinterfaces in the presence of bovine albumin, Analyst 138 (20) (2013) 6192–6196.
[45] G. Herzog, V. Kam, D.W.M. Arrigan, Electrochemical behaviour of haemoglobin at the liquid/liquid interface, Electrochim. Acta 53 (24) (2008) 7204–7209.
[46] S. O'Sullivan, D.W.M. Arrigan, Electrochemical behaviour of myoglobin at an array of microscopic liquid–liquid interfaces, Electrochim. Acta 77 (2012) 71–76.
[47] Y. Imai, T. Sugihara, T. Osakai, Electron transfer mechanism of cytochrome c at the oil/water interface as a biomembrane model, J. Phys. Chem. B 116 (1) (2012) 585–592.
[48] E. Alvarez de Eulate, S. O'Sullivan, D.W.M. Arrigan, Electrochemically induced formation of cytochrome c oligomers at soft interfaces, Chemelectrochem 4 (4) (2017) 898–904.
[49] H. Nagatani, T. Ueno, T. Sagara, Spectroelectrochemical analysis of ion-transfer and adsorption of the PAMAM dendrimer at a polarized liquid| liquid interface, Electrochim. Acta 53 (22) (2008) 6428–6433.
[50] H. Nagatani, M. Fujisawa, H. Imura, Mechanistic analysis of ion association between dendrigraft poly-l-lysine and 8-anilino-1-naphthalenesulfonate at liquid| liquid interfaces, Langmuir 34 (10) (2018) 3237–3243.
[51] T. Takami, S. Kanai, Y. Nishiyama, H.J. Lee, H. Nagatani, Transfer mechanism of anthracycline antibiotics and their ion association with PAMAM dendrimer at Liquid| liquid interfaces, Chemelectrochem 9 (13) (2022) e202200359.
[52] M. Calderon, L.M. Monzón, M. Martinelli, A.V. Juarez, M.C. Strumia, L.M. Yudi, Electrochemical study of a dendritic family at the water/1, 2-dichloroethane interface, Langmuir 24 (12) (2008) 6343–6350.
[53] G. Herzog, S. Flynn, C. Johnson, D.W.M. Arrigan, Electroanalytical behavior of poly-l-lysine dendrigrafts at the interface between two immiscible electrolyte solutions, Anal. Chem. 84 (13) (2012) 5693–5699.
[54] L. Poltorak, K. Morakchi, G. Herzog, A. Walcarius, Electrochemical characterization of liquid-liquid micro-interfaces modified with mesoporous silica, Electrochim. Acta 179 (2015) 9–15.

[55] M. Li, P. He, Z. Yu, S. Zhang, C. Gu, X. Nie, Y. Gu, X. Zhang, Z. Zhu, Y. Shao, Investigation of dendrimer transfer behaviors at the micro-water/1, 2-dichloroethane interface facilitated by dibenzo-18-crown-6, Anal. Chem. 93 (3) (2020) 1515–1522.
[56] K. Kowalewska, T. Rodriguez-Prieto, S. Skrzypek, J. Cano, R.G. Ramírez, L. Poltorak, Electroanalytical study of five carbosilane dendrimers at the interface between two immiscible electrolyte solutions, Analyst 146 (4) (2021) 1376–1385.
[57] A. Berduque, M.D. Scanlon, C.J. Collins, D.W.M. Arrigan, Electrochemistry of non-redox-active poly (propylenimine) and poly (amidoamine) dendrimers at liquid− liquid interfaces, Langmuir 23 (13) (2007) 7356–7364.
[58] S. Liu, Q. Li, Y. Shao, Electrochemistry at micro- and nanoscopic liquid/liquid interfaces, Chem. Soc. Rev. 40 (5) (2011) 2236–2253.
[59] Y. Shao, M.V. Mirkin, Fast kinetic measurements with nanometer-sized pipets. Transfer of potassium ion from water into dichloroethane facilitated by dibenzo-18-crown-6, J. Am. Chem. Soc. 119 (34) (1997) 8103–8104.
[60] G.J. Islam, S. Zannah, Scope of Electrochemistry at Liquid/liquid Micro-interfaces, Dhaka University Journal of Science, 2022, pp. 186–193.
[61] H.J. Lee, P.D. Beattie, B.J. Seddon, M.D. Osborne, H.H. Girault, Amperometric ion sensors based on laser-patterned composite polymer membranes, J. Electroanal. Chem. 440 (1) (1997/12/20/, 1997) 73–82.
[62] G.J. Islam, D.W.M. Arrigan, Voltammetric selectivity in detection of ionized perfluoroalkyl substances at micro-interfaces between immiscible electrolyte solutions, ACS Sens. 7 (10) (2022) 2960–2967.
[63] F. Kivlehan, Y.H. Lanyon, D.W.M. Arrigan, Electrochemical study of insulin at the polarized liquid− liquid interface, Langmuir 24 (17) (2008) 9876–9882.
[64] P.K. Maiti, T. Çağın, S.-T. Lin, W.A. Goddard, Effect of solvent and pH on the structure of PAMAM dendrimers, Macromolecules 38 (3) (2005) 979–991.
[65] R. Kharwade, S. More, A. Warokar, P. Agrawal, N. Mahajan, Starburst pamam dendrimers: synthetic approaches, surface modifications, and biomedical applications, Arab. J. Chem. 13 (7) (2020) 6009–6039.
[66] M.A. Méndez, B. Su, H.H. Girault, Voltammetry for surface-active ions at polarisable liquid| liquid interfaces, J. Electroanal. Chem. 634 (2) (2009) 82–89.
[67] P. Beattie, A. Delay, H. Girault, Investigation of the kinetics of assisted potassium ion transfer by dibenzo-18-crown-6 at the micro-ITIES by means of steady-state voltammetry, J. Electroanal. Chem. 380 (1–2) (1995) 167–175.
[68] V.A. Jiménez, J.A. Gavín, J.B. Alderete, Scaling trend in diffusion coefficients of low generation G0–G3 PAMAM dendrimers in aqueous solution at high and neutral pH, Struct. Chem. 23 (1) (2012) 123–128.
[69] P.K. Maiti, B. Bagchi, Diffusion of flexible, charged, nanoscopic molecules in solution: size and pH dependence for PAMAM dendrimer, J. Chem. Phys. 131 (21) (2009).
[70] B. Fritzinger, U. Scheler, Scaling behaviour of PAMAM dendrimers determined by diffusion NMR, Macromol. Chem. Phys. 206 (13) (2005) 1288–1291.
[71] M.M. Sanagi, S.L. Ling, Z. Nasir, D. Hermawan, W.A. Wan Ibrahim, A.A. Naim, Comparison of signal-to-noise, blank determination, and linear regression methods for the estimation of detection and quantification limits for volatile organic compounds by gas chromatography, J. AOAC Int. 92 (6) (2009) 1833–1838.
[72] A. Shrivastava, V.B. Gupta, Methods for the determination of limit of detection and limit of quantitation of the analytical methods, Chron. Young Sci 2 (1) (2011) 21–25.